

Note that all line numbers in our responses refer to the version with tracked comments included in this document. Line numbers from the reviewers refer to the original manuscript.

Reviewer #1

We thank the reviewer for their comments. Below, we detail our responses.

64-65. As a single number to quantify the spread, the standard deviation would also be helpful.

We have added 5-95% confidence intervals throughout the paper.

66. Why do you use only a single decade, rather than all the data, for instance by dividing the dataset into two or using regression (cf Barnes and Barnes, 2015, 10.1175/JCLI-D-15-0032.1)? A single decade would be less precise. You could estimate the statistical uncertainty incurred from the control run.

We calculate ECS using this approach because this is the way most ECS calculations based on the 20th-century observational record are done. Thus, our results can therefore directly provide insight into the impact of variability in the observational estimates of ECS.

The reviewer is correct that using more than a decade might affect the results. If one used the difference between the averages of the first and last 20 years, the range in λ declines from 0.87 W/m²/K to 0.48 W/m²/K. Using longer averaging periods does not further decrease the range. We now mention this in the paper (line 67).

118. It would be useful to remark here that 16 years is chosen to match the CERES dataset, because that was mentioned some lines above (103-104), where it appears actually to be 17 years and 5 months long.

We have added a statement that the segmentation of the data is done to match the CERES record (line 134). We have also updated the paper to segment the data into 17-year segments to more closely match CERES.

119, 196. Why are monthly anomalies used here, rather than annual? Does it make a difference?

We do this to facilitate the comparison with the CERES regressions, which also uses monthly data. The reason most analyses with CERES data are done with monthly data is because using annual data means there's only 17 data points, and the uncertainties end up being very large. Issues involved in annual vs. monthly regressions are discussed in some detail in Forster (2016, 10.1146/annurev-earth-060614-105156).

167. Again, the standard deviation would be helpful, and could be compared with lines 64-65.

Added.

173, 175. You could give standard errors of the mean for each of these two numbers, and judge the significance of their difference.

We have added the 5-95% confidence intervals to all of these numbers.

174, 175. "analysis" and "calculated" - by what method? From the slope of R against Delta T?

We have clarified the text that we use the method of Gregory et al. (2004), where annual average R is regressed against T, and the slope of the curve is an estimate of λ or Θ (line 194)

204. "agrees" in what sense?

We have changed the sentence to read: "We find that the 15 models whose average short-term Θ falls within the uncertainty of Θ estimated from CERES observations have ECS values ranging from 2.0-3.9 K, with an average of 2.9 K." (line 247)

218. I would say that this is "one source" of the spread, which is not eliminated, but only reduced, by using Theta instead.

We believe that this sentence is phrased correctly. The spread in our estimate from the ensemble is due to the construction of the energy-balance equation. Unlike observational analyses, we know everything else perfectly. Using our revised energy balance equation does not completely solve the problem, but it is an improvement.

233. Why is this material an appendix, rather than being incorporated in the main text?

We felt that this material would not be interesting to most readers, so we put it in the appendix. In retrospect, perhaps that was a bad decision. At this stage in the paper's review cycle, we hesitate to move material around. We can, however, if the reviewer or editor insists.

Reviewer #2

We thank the reviewer for their comments. In this document, we detail our responses.

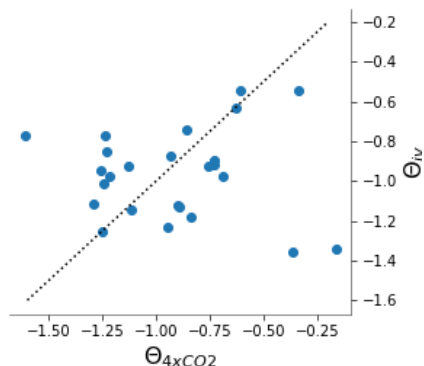
1) It would be helpful to provide a little more physical motivation for the choice of tropical 500 hPa temperature. I see some good reasons why mid-tropospheric temperature should work better (e.g., it should scale better with LR, WV and LW cloud feedbacks), but I don't think this was discussed anywhere. Why use tropical temperature rather than global-mean? Is there a physical rationale, or did this simply work better in MPI-ESM?

Also, although mid-tropospheric temperature clearly works better for the overall feedback, I expect the scaling with Ta might actually be a worse choice for some individual feedback processes (e.g. surface albedo, marine low cloud). This might be worth discussing briefly.

A: To address this, we have added a paragraph to the paper beginning on line 221.

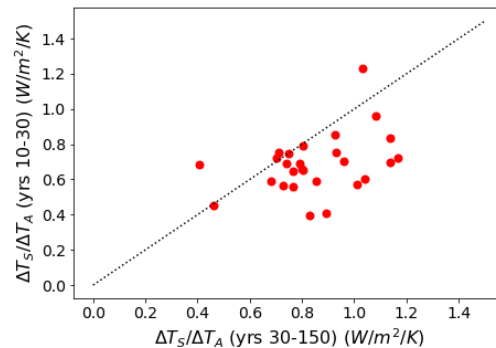
2) A key result is that the revised feedback parameter θ more accurately estimates the “true” feedback strength under CO_2 forcing. This is shown to be the case in MPI-ESM (L172-176). However, does this hold for CMIP5 models in general? I.e., do the values of θ estimated in control runs correlate well with those in $4\times\text{CO}_2$?

A: This is not a claim we make in the paper, although one might infer it from the MPI model. Indeed, there is *some* correlation between short-term and long-term θ in the CMIP5 ensemble, as seen here:



So if most of the curvature in the relationship between radiative response and temperature goes away with the revised framework (Fig. 6), I expect there must be some curvature in the T_A versus T_S relationship in 4xCO2 runs. Can the authors confirm this?

Confirmed.



Caption. Scatterplot of slope of ΔT_S vs. ΔT_A in CMIP5 abrupt4xCO2 runs. Each point represents one model. The dotted line is the 1:1 line. The subscripts (10-30, 30-150) indicate the years of the run from which the slopes are calculated.

We've added a sentence to the paper mentioning that there is curvature in T_A vs T_S relation: "The lack of curvature in the Θ calculations means there is curvature in the relation between T_A and T_S in the models." (line 216)

4) I expect the T_S/T_A ratio cannot be reliably estimated from historical runs in the presence of large variability (for the same reason that λ cannot be reliably estimated - because of the pattern effect). So we must rely on models to estimate this ratio under future global warming, meaning that it will be important to understand how future patterns of surface warming will develop. I suggest the authors discuss this briefly, for example in the conclusions.

We have added a sentence to the paper mentioning this point: "This also emphasizes the need to improve our understanding of the factors that control $\Delta T_S / \Delta T_A$, as well as how future patterns of surface warming will evolve." (line 218)

Other minor comments:

I suggest using colors in Fig. 6, rather than dark grey and black.

Done

L223: Cite Andrews and Webb 2018 - For future reference, it would be useful to mention the value of θ estimated from observations (horizontal dashed bar in Fig. 7a).

Done.

1 **The influence of internal variability on Earth's energy balance framework and implications for**
2 **estimating climate sensitivity**

3 Andrew E. Dessler^{1*}, Thorsten Mauritsen², Bjorn Stevens²

4 ¹ Dept. of Atmospheric Sciences, Texas A&M University, College Station, TX 77843

5 ² Max Planck Institute for Meteorology, Bundesstraße 53, 20146 Hamburg, Germany

6 *Correspondence to: adessler@tamu.edu, 979-862-1427

7 Keywords: Climate sensitivity, climate variability, energy balance

8 **Abstract:** Our climate is constrained by the balance between solar energy absorbed by the
9 Earth and terrestrial energy radiated to space. This energy balance has been widely used to
10 infer equilibrium climate sensitivity (ECS) from observations of 20th-century warming. Such
11 estimates yield lower values than other methods and these have been influential in pushing
12 down the consensus ECS range in recent assessments. Here we test the method using a 100-
13 member ensemble of the MPI-ESM1.1 climate model simulations of the period 1850-2005 with
14 known forcing. We calculate ECS in each ensemble member using energy balance, yielding
15 values ranging from 2.1 to 3.9 K. The spread in the ensemble is related to the central
16 hypothesis in the energy budget framework: that global average surface temperature
17 anomalies are indicative of anomalies in outgoing energy (either of terrestrial origin or reflected
18 solar energy). We find that assumption is not well supported over the historical temperature
19 record in the model ensemble or more recent satellite observations. We find that framing
20 energy balance in terms of 500-hPa tropical temperature better describes the planet's energy
21 balance.

22

23 **The problem**

24 When an energy imbalance is imposed, such as by adding a greenhouse gas to the atmosphere,
25 the climate will shift in such a way to eliminate the energy imbalance. This process is
26 embodied in the traditional linearized energy balance equation:

27
$$R = F + \lambda T_s \quad (1)$$

28 where the forcing F is an imposed energy imbalance, T_s is the global average surface
29 temperature, and λ relates changes in T_s to a change in net top-of-atmosphere (TOA) flux
30 (Gregory et al., 2002; Dessler and Zelinka, 2014). R is the resulting TOA flux imbalance from the
31 combined forcing and response. All quantities are deviations from an equilibrium base state,
32 usually the pre-industrial climate. Equilibrium climate sensitivity (hereafter ECS, the equilibrium
33 warming in response to a doubling of CO_2) is equal to $-F_{2\times\text{CO}_2}/\lambda$, where $F_{2\times\text{CO}_2}$ is the forcing from
34 doubled CO_2 .

35 Many investigators (e.g., Gregory et al., 2002; Annan and Hargreaves, 2006; Otto et al., 2013;
36 Lewis and Curry, 2015; Aldrin et al., 2012; Skeie et al., 2014; Forster, 2016) have used Eq. 1
37 combined with estimates of R , F , and T_s to estimate λ :

38
$$\lambda = \Delta(R-F)/\Delta T_s \quad (2)$$

39 where Δ indicates the change between the start of the historical period (usually the mid to late
40 nineteenth century) and a recent period. These calculations result in values of λ near
41 $-2 \text{ W/m}^2/\text{K}$ and appear to rule out ECS larger than $\sim 4 \text{ K}$ (Stevens et al., 2016). The substantial
42 likelihood of an ECS below 2 K implied by these calculations led the IPCC Fifth Assessment
43 Report to extend their lower bound on *likely* values of ECS to 1.5 K (Collins et al., 2013).

44 We test this energy balance methodology through a perfect model experiment consisting of an
45 analysis of a 100-member ensemble of runs of the MPI Earth System Model, MPI-ESM1.1. This
46 is the latest coupled climate model from the Max Planck Institute for Meteorology and consists
47 of the ECHAM6.3 atmosphere and land model coupled to the MPI-OM ocean model. The
48 atmospheric resolution is T63 spectral truncation, corresponding to about 200 km , with 47

49 vertical levels, whereas the ocean has a nominal resolution of about 1.5 degrees and 40 vertical
50 levels. MPI-ESM1.1 is a bug-fixed and improved version of the MPI-ESM used during CMIP5
51 (Giorgetta et al., 2013) and nearly identical to the MPI-ESM1.2 (Mauritsen et al., 2018) model
52 being used to provide output to CMIP6, except that the historical forcings are from the MPI-
53 ESM.

54 Each of the 100 members simulates the years 1850-2005 (Fig. 1) and use the same evolution of
55 historical natural and anthropogenic forcings. The members differ only in their initial
56 conditions —each starts from a different state sampled from a 2000-year control simulation.
57 We calculate effective radiative forcing F for the ensemble by subtracting top-of-atmosphere
58 flux R in a run with climatological sea surface temperatures (SSTs) and a constant pre-industrial
59 atmosphere from average R from an ensemble of three runs using the same SSTs but the time-
60 varying atmospheric composition used in the historical runs (Hansen et al., 2005; Forster et al.,
61 2016). The three-member ensemble begins with perturbed atmospheric states. We estimate
62 $F_{2\times\text{CO}_2}$ using the same approach in a set of fixed SST runs in which CO_2 increases at 1% per year,
63 which yields a $F_{2\times\text{CO}_2}$ value of 3.9 W/m^2 .

64 We calculate λ using Eq. 2 for each ensemble member, producing values ranging from -1.88 to
65 $-1.01 \text{ W/m}^2/\text{K}$ (5-95% range -1.63 to $-1.17 \text{ W/m}^2/\text{K}$), with an ensemble median of $-1.43 \text{ W/m}^2/\text{K}$
66 (Fig. 2a). In this calculation, $\Delta(R-F)$ and ΔT_s are the average difference between the first and last
67 decade of each run. The spread in λ depends to some extent on how the calculation is set up
68 — if one used the difference between the averages of the first and last 20 years, for example,
69 the range in λ declines from $0.87 \text{ W/m}^2/\text{K}$ to $0.48 \text{ W/m}^2/\text{K}$. Using longer averaging periods does
70 not further decrease the range.

71 We also calculate $\text{ECS} = -F_{2\times\text{CO}_2}/\lambda$ for each ensemble member, producing values ranging from
72 2.08 to 3.87 K (5-95% range 2.39 to 3.34 K) (Fig. 2b), with an ensemble median of 2.72 K . Thus,
73 our analysis shows that λ and ECS estimated from the historical record can vary widely simply
74 due to internal variability. Given that we have only a single realization of the 20th century, we
75 should not consider estimates based on the historical period to be precise — even with perfect
76 observations. This supports previous work that also emphasized the impact of internal

Deleted: average

Deleted: average

Deleted: 6

Deleted: ¶

With respect to precision of the estimates

82 variability on estimates of λ and ECS (Huber et al., 2014; Andrews et al., 2015; Zhou et al., 2016;
83 Gregory and Andrews, 2016).

84 Previous researchers have questioned whether the historical record provides an accurate
85 measure of λ and ECS, and we can check this by comparing the ensemble values to ECS
86 estimates from a 2xCO₂ run of the MPI-ESM1.2, which is physically very close to MPI-ESM1.1,
87 An abrupt 2xCO₂ run yields an ECS of 2.93 K in response to an abrupt doubling of CO₂
88 (estimated by regressing years 100-1000 of a 1000-year run) — 8% larger than the ensemble
89 median. This is in line with the 10% difference in ECS estimated by Mauritsen and Pincus (2017)
90 to arise from the average CMIP5 model time-dependent feedback, but smaller than suggested
91 in other recent studies of ECS in transient climate runs (e.g., Armour, 2017; Proistosescu and
92 Huybers, 2017).

93 Thus, there are a number of issues that need to be considered when interpreting estimates of λ
94 and ECS derived from the historical period. In addition to the precision and accuracy issues
95 discussed above, it also includes the large and evolving uncertainty in forcing over the 20th
96 century (Forster, 2016), different forcing efficacies of greenhouse gases and aerosols (Shindell,
97 2014; Kummer and Dessler, 2014), and geographically incomplete or inhomogeneous
98 observations (Richardson et al., 2016).

99 **Why are estimates using the traditional energy balance approach imprecise?**

100 In this section, we explain the physical process by which internal variability leads to the large
101 spread in λ and ECS estimated from the ensemble. We begin by observing that Eqs. 1 and 2
102 parameterize R-F in terms of global average surface temperature, T_s . In model runs with strong
103 forcing driving large warming, such as abrupt 4xCO₂ simulations, there is indeed a strong
104 correlation between these variables (e.g., Gregory et al., 2004). However, because R-F in such
105 runs is dominated by a monotonic trend, correlations will exist with any geophysical field that
106 also exhibits a monotonic trend, regardless of whether there is a physical connection between
107 the fields. Thus, one should not take the correlation between R-F and T_s in these runs as
108 proving causality.

Deleted: average

Deleted: and the changes between the MPI-ESM1.1 and MPI-ESM1.2 are not believed to be important for its climate sensitivity

Deleted: 6

Deleted: average

115 If T_s is a good proxy for the response R-F, we would expect to also see a correlation in
116 measurements dominated by interannual variations. Observational data allow us to test this
117 hypothesis. We use observations of R from the Clouds and the Earth's Radiant Energy System
118 (CERES) Energy Balanced and Filled product (ed. 4) (Loeb et al., 2009), which cover the period
119 March 2000 to July, 2017. Our sign convention throughout the paper is that downward fluxes
120 are positive. Temperatures come from the European Centre for Medium Range Weather
121 Forecasts (ECMWF) Interim Re-Analysis (ERAi) (Dee et al., 2011). We assume forcing changes
122 linearly over this time period and account for it by detrending ΔR and ΔT anomaly time series
123 using a linear least-squares fit to remove the long-term trend.

124 These data show that ΔR is poorly correlated with ΔT_s in response to interannual variability (Fig.
125 3a), as has been noted many times in the literature; see, e.g., Sect. 5 of Forster (2016). In
126 particular, the low correlation coefficient tells us that ΔT_s explains little of the variance in ΔR .
127 Using explicit estimates of forcing or other temperature datasets (e.g., MERRA-2) yield the
128 same result.

129 GCMs that submitted output to the 5th phase of the Coupled Model Intercomparison Project
130 (CMIP5) (Taylor et al., 2012) also show this poor correlation. To demonstrate this, we have
131 calculated the correlation coefficient between ΔT_s and ΔR in CMIP5 pre-industrial control runs
132 (these are runs for which forcing $F = 0$). To facilitate comparison with the CERES data, as well as
133 avoid any issues with long-term drift in the control runs, we break each run into 17-year
134 segments to match the length of the CERES data and calculate the correlation coefficient of
135 monthly anomalies of ΔR and ΔT_s for each segment. Fig. 4 shows that the correlation between
136 ΔR and ΔT_s in the models is similar to that from the CERES analysis.

137 Recent work provides an explanation: the response of $\Delta(R-F)$ to a particular ΔT_s is determined
138 not only by the global average magnitude, but also by the pattern of warming (Armour et al.,
139 2013; Andrews et al., 2015; Gregory and Andrews, 2016; Zhou et al., 2016, 2017; Andrews and
140 Webb, 2018). During El Nino cycles that dominate the observations in Fig. 3, the spatial pattern
141 of warm and cool regions changes, leading to responses in $\Delta(R-F)$ that do not scale cleanly with
142 ΔT_s — something Stevens et al. (2016) refer to as “pattern effects”

Deleted: 6

Deleted: (2016)

145 To demonstrate how this also generates the spread in λ in the model ensemble (Fig. 2a), we
146 calculate the local response λ_r in three equal-area regions (90°S-19.4°S, 19.4°S-19.4°N, 19.4°N-
147 90°N). We define λ_r as the regional analog to λ (Eq. 2):

$$148 \quad \lambda_r = \Delta(R-F)_r / \Delta T_{s,r} \quad (3)$$

149 where the “r” subscript indicates a regional average value.

150 We find that λ_r varies between the regions (Fig. 5). This means that different ensemble
151 members with similar global average ΔT_s but different patterns of surface warming produce
152 different values of global average $\Delta(R-F)$, thereby leading to spread in the estimated λ among
153 the ensemble members. We also see strong variability in λ_r within each region, suggesting that
154 how the warming is distributed within the region also drives some of the spread in estimated λ
155 in the ensemble.

156 This explanation is consistent with analyses showing that λ changes during transient runs as the
157 pattern of surface temperature evolves (Senior and Mitchell, 2000; Armour et al., 2013;
158 Andrews et al., 2015; Gregory and Andrews, 2016; Stevens et al., 2016). In our model
159 ensemble, however, the pattern changes are caused by internal variability rather than differing
160 regional heat capacities that cause some regions to warm more slowly than others during
161 forced warming.

162 **A better way to describe energy balance**

163 Our analysis demonstrates limitations of the conventional energy balance framework (Eq. 1). It
164 has been previously noted that ΔR correlates better with tropospheric temperatures than ΔT_s
165 (Murphy, 2010; Spencer and Braswell, 2010; Trenberth et al., 2015). Recent analyses have also
166 stressed the importance of atmospheric temperatures — through its influence on lapse rate —
167 as providing a fundamental control on the planet’s energy budget (Zhou et al., 2016; Ceppi and
168 Gregory, 2017). Based on this, we test a new energy balance framework constructed using the
169 temperature of the tropical atmosphere:

170 $R - F = \Theta T_A$ (4)

171 where T_A is the tropical average (30°N-30°S) 500-hPa temperature and Θ relates this quantity to
172 R-F. R and F are the same global average quantities they were in equation 1. ECS can be
173 expressed in terms of Θ :

174 $ECS = -\frac{\Delta F_{2 \times CO_2}}{\Theta} \frac{\Delta T_S}{\Delta T_A}$ (5)

175 where ΔT_S and ΔT_A are the equilibrium changes in these quantities in response to doubled CO_2 .
176 The CMIP5 ensemble average ratio $\Delta T_S/\Delta T_A$ is 0.86 ± 0.10 ($\pm 1\sigma$), where Δ represents the average
177 difference between the first and last decades of the abrupt $4xCO_2$ runs.

178 Support for Eq. 4 can be found in the observations: ΔR shows a tighter correlation with ΔT_A than
179 with ΔT_S in observations (Figs. 3a vs. 3b). [CMIP5 models also show this \(Fig. 4\)](#). Given that the
180 slope of these plots can be taken as estimates of Θ and λ , the tighter correlation leads to more
181 accurate estimates of Θ than λ , both in absolute and relative terms.

182 Turning to the model ensemble, we next demonstrate that Θ is a more precise metric than λ .
183 We do this by calculating Θ [$= \Delta(R-F)/\Delta T_A$] in each ensemble member, yielding values ranging
184 from -1.18 to -0.89 W/m²/K ([5-95% range -1.16 to -0.92 W/m²/K](#)), with an ensemble [median](#) of
185 -1.04 W/m²/K (Fig. 2a). There is clearly less variability in Θ among the ensemble members than
186 for λ . This reflects less variability in the regional response Θ_r ($= \Delta(R-F)_r/\Delta T_{A,r}$) than [in](#) λ_r (Fig. 5),
187 as well as less variability within the regions. We therefore conclude that interannual variability
188 has less of an impact on Θ than λ . We show additional evidence for the superior precision of Θ
189 in the Appendix.

190 As far as accuracy goes, we can compare Θ in the ensemble over the historical period to Θ in
191 response to much larger warming. The ensemble [median of](#) Θ from the historic period ([Fig. 2](#)),
192 -1.04 \pm 0.01 W/m²/K ([5-95% confidence interval](#)), is close to the value obtained from an analysis
193 of the first 150 years of an abrupt $4xCO_2$ run of the same model, $\Theta = -1.03 \pm 0.04$ W/m²/K, as
194 well as Θ calculated from all 2600 years of this run, $\Theta = -1.00 \pm 0.01$ W/m²/K ([values from the](#)
195 [4xCO₂ runs are all obtained using the Gregory method \(Gregory et al., 2004\) using annual](#)

Deleted: ;

Deleted: t

Deleted: average

Deleted: average

Deleted: 4

201 average R and temperatures). On the other hand, λ changes substantially in the 4xCO₂ run as
202 the climate warms: $\lambda = -1.36 \pm 0.07$ W/m²/K when calculated from the first 150 years, but $\lambda =$
203 -0.95 ± 0.01 W/m²/K from all 2600 years of that run.

Deleted: .

204 We can verify this result in the CMIP5 abrupt 4xCO₂ ensemble. It has been previously
205 demonstrated that plots of R-F vs. T_s do not trace straight lines as the climate warms (Andrews
206 et al., 2015; Rugenstein et al., 2016; Rose and Rayborn, 2016; Armour, 2017), so λ and ECS
207 calculated in a single model run may depend on the portion of the run selected. In the CMIP5
208 abrupt 4xCO₂ ensemble, for example, average λ calculated by regressing years 10-30 (λ_{10-30}) is
209 more negative than λ calculated from years 30-150 (λ_{30-150}) by 0.49 W/m²/K (Fig. 6).

Deleted: 50

210 Several explanations for this have been advanced, most prominently that λ is function of the
211 pattern of surface warming (Senior and Mitchell, 2000; Armour et al., 2013; Andrews et al.,
212 2015; Gregory and Andrews, 2016; Zhou et al., 2016; Stevens et al., 2016). Using Θ largely
213 eliminates this pattern effect: Θ_{10-30} and Θ_{30-150} have an average difference of 0.13 W/m²/K for
214 the CMIP5 ensemble (Fig. 6). Thus, we find additional evidence that Θ tends to be similar for
215 different amounts and patterns of warming.

Deleted: 6

216 The lack of curvature in the Θ calculations means there is curvature in the relation between T_A
217 and T_s in the models. Thus, the pattern effect's impact on ECS calculations shifts from λ in the
218 traditional framework to the $\Delta T_s / \Delta T_A$ term in Eq. 4. This also emphasizes the need to improve
219 our understanding of the factors that control $\Delta T_s / \Delta T_A$, as well as how future patterns of surface
220 warming will evolve.

221 There are several plausible reasons why T_A may control R better than T_s. It seems likely that
222 several of the feedbacks — e.g., lapse rate, water vapor, longwave cloud — should be more
223 strongly influenced by atmospheric temperatures than T_s. More recently, it has been shown
224 that atmospheric temperatures also play a key role in regulating low clouds (Zhou et al., 2016,
225 2017), thereby influencing the shortwave cloud feedback. This is also consistent with Ceppi et
226 al. (2017), who identified a dependence of ECS on atmospheric stability in models. We have
227 not further investigated this — ultimately, our use of T_A in Eq. 4 is based on observations

231 (Murphy, 2010; Spencer and Braswell, 2010; Trenberth et al., 2015) that it correlates well with
232 R. Other metrics, such as global average atmospheric temperature work almost as well.
233 Clearly, further investigations on how to best describe the Earth's energy balance are
234 warranted.

235 Finally, one of our ultimate goals for this revised framework is to help produce better estimates
236 of ECS. We are working on a detailed analysis of ECS based on this framework and will publish
237 that in a follow-on paper, but we briefly show here how the advantages of the revised energy
238 balance framework may be leveraged to do this. Fig. 7a shows Θ calculated from control runs
239 of 25 CMIP5 models. To calculate Θ in the control runs, we break each control run into 17-year
240 segments and calculate monthly anomalies of ΔR and ΔT_A during each segment. Then, we
241 calculate Θ for each segment as the slope of the regression of ΔR vs. ΔT_A for that segment.
242 Thus, for each control run, we generate a large number of estimates of Θ . The value in Fig. 7a is
243 the average of these individual values.

244 Fig. 7b shows the ECS of these models, calculated from the first 150 years of the abrupt 4xCO₂
245 runs using the Gregory method. If we assume that models with more accurate simulation of
246 short-term Θ produce more accurate estimates of ECS (Brown and Caldeira, 2017; Wu and
247 North, 2002), then we can use Figs. 7a and 7b to constrain ECS. We find that the 15 models
248 whose average short-term Θ falls within the uncertainty of Θ estimated from CERES
249 observations have ECS values ranging from 2.0-3.9 K, with an average of 2.9 K. This excludes
250 many of the highest ECS models, a result consistent with other analyses (Cox et al., 2018; Lewis
251 and Curry, 2015).

252 It would not have been possible to draw this conclusion with the conventional energy balance
253 framework. Fig. 7c shows the comparison between λ from the control runs (calculated the
254 same way Θ was calculated) and CERES observations. Because of the much larger uncertainty
255 in the observational estimate of short-term λ , almost all models fall within the observational
256 range, thereby prohibiting any constraint on the ECS range.

Deleted: 6

Deleted: (Gregory et al., 2004)

Deleted: agrees with the

260 It may also be possible to use the relation between short-term and long-term Θ as an emergent
261 constraint to convert short-term observations to the long-term response. There is some scatter
262 in the relation in the CMIP5 ensemble, however, so more analysis of how these relate is likely
263 required before ECS can be constrained in this way.

264 **Conclusions**

265 We have estimated ECS in each of a 100-member climate model ensemble using the same
266 energy-balance constraint used by many investigators to estimate ECS from 20th-century
267 historical observations. We find that the method is imprecise — the estimates of ECS range
268 from 2.1 to 3.9 K (Fig. 2), with some ensemble members far from the model's true value of 2.9
269 K. Given that we only have a single ensemble of reality, one should recognize that estimates of
270 ECS derived from the historical record may not be a good estimate of our climate system's true
271 value.

Deleted: this suggests that some skepticism is appropriate when considering

272 The source of the imprecision relates to the construction of the traditional energy balance
273 equation (Eq. 1). In it, the response of TOA net flux (R-F) is parameterized in terms of global
274 average surface temperature (T_s). Recent research has suggested that the response is not just
275 determined by the magnitude of T_s , but includes other factors, such as the pattern of T_s (e.g.,
276 Armour et al., 2013; Andrews et al., 2015; Gregory and Andrews, 2016; Zhou et al., 2017) or the
277 lapse rate (e.g., Zhou et al., 2017; Ceppi and Gregory, 2017; Andrews and Webb, 2018). As a
278 result, two ensemble members with the same ΔT_s can have different climate responses, $\Delta(R-$
279 $F)$, leading to spread in the inferred λ .

280 The lack of a direct relationship between T_s and radiation balance suggests that it may be
281 profitable to investigate alternative formulations. We test parameterizing the response in terms
282 of 500-hPa tropical temperature (Eq. 4) and find that it is superior in many ways. Ultimately,
283 how investigators describe the energy balance of the planet will depend on the problem and
284 the available data. The surface temperature is indeed special, so the traditional framework
285 may be preferred for some problems. But investigators may find that the alternatives are
286 superior for certain problems, for instance constraining Earth's climate sensitivity.

289 Appendix

290 It has been previously noted in analyses of the historical record that λ exhibits significant
291 interdecadal variability (Andrews et al., 2015; Gregory and Andrews, 2016; Zhou et al., 2016).

292 We can reproduce this in a 2000-year control run (a run with fixed pre-industrial boundary
293 conditions) of the MPI-ESM1.1 model. Fig. 8 shows λ calculated in a sliding 17-year window
294 and confirms significant temporal variability in λ . We can similarly calculate Θ and find that
295 temporal variability in Θ is substantially smaller (Fig. 8).

296 This result is reproduced in the CMIP5 control models. Fig. 9 plots the standard deviation of
297 each CMIP5 model's set of short-term λ divided by the standard deviation of that model's set of
298 short-term Θ (as described previously, we calculate time series of short-term λ and Θ values for
299 each model by regressing anomalies in a 17-year sliding window of the control runs). All of the
300 models fall above 1, demonstrating that there is less variability in the Θ time series than in the
301 λ time series in every climate model. This confirms that Θ is more robust with respect to
302 internal variability than λ . It also suggests that Θ estimated from the satellite data (Fig. 3)
303 should be considered a better estimate of the climate system's long-term value than λ
304 estimated from the same data set.

305 **Acknowledgements:** This work was supported by NSF grant AGS-1661861 to Texas A&M
306 University. This work was initiated while AED was on Faculty Development Leave from Texas
307 A&M during the Fall of 2016; he thanks Texas A&M and the Max Planck Institut für
308 Meteorologie for supporting this research. Computational resources were made available by
309 Deutsches Klimarechenzentrum (DKRZ) through support from German Federal Ministry of
310 Education and Research (BMBF), and by the Swiss National Supercomputing Centre (CSCS).

312
313 Code and links to data can be found at
314 <https://github.com/aedessler/DesslerMauritsenStevens18>
315

Deleted: 6

Deleted: 6

Deleted: ::::::::::::::::::::Page Break::::::::::::::::::

Deleted: completed

320 **References**

- 321 Aldrin, M., Holden, M., Guttorp, P., Skeie, R. B., Myhre, G., and Berntsen, T. K.: Bayesian
322 estimation of climate sensitivity based on a simple climate model fitted to observations of
323 hemispheric temperatures and global ocean heat content, *Environmetrics*, 23, 253-271,
324 10.1002/env.2140, 2012.
- 325 Andrews, T., Gregory, J. M., and Webb, M. J.: The dependence of radiative forcing and feedback
326 on evolving patterns of surface temperature change in climate models, *J. Climate*, 28,
327 1630-1648, 10.1175/JCLI-D-14-00545.1, 2015.
- 328 Andrews, T., and Webb, M. J.: The Dependence of Global Cloud and Lapse Rate Feedbacks on
329 the Spatial Structure of Tropical Pacific Warming, *J. Climate*, 31, 641-654, 10.1175/jcli-d-17-
330 0087.1, 2018.
- 331 Annan, J. D., and Hargreaves, J. C.: Using multiple observationally-based constraints to estimate
332 climate sensitivity, *Geophys. Res. Lett.*, 33, 10.1029/2005gl025259, 2006.
- 333 Armour, K. C., Bitz, C. M., and Roe, G. H.: Time-varying climate sensitivity from regional
334 feedbacks, *J. Climate*, 26, 4518-4534, 10.1175/jcli-d-12-00544.1, 2013.
- 335 Armour, K. C.: Energy budget constraints on climate sensitivity in light of inconstant climate
336 feedbacks, *Nature Clim. Change*, 7, 331-335, 10.1038/nclimate3278, 2017.
- 337 Brown, P. T., and Caldeira, K.: Greater future global warming inferred from Earth's recent
338 energy budget, *Nature*, 552, 10.1038/nature24672, 2017.
- 339 Ceppi, P., and Gregory, J. M.: Relationship of tropospheric stability to climate sensitivity and
340 Earth's observed radiation budget, *Proc. Natl. Acad. Sci.*, 10.1073/pnas.1714308114, 2017.
- 341 Collins, M., et al.: Long-term climate change: Projections, commitments and irreversibility, in:
342 *Climate Change 2013: The Physical Science Basis. Contribution of Working Group I to the*
343 *Fifth Assessment Report of the Intergovernmental Panel on Climate Change*, edited by:
344 Stocker, T. F., Qin, D., Plattner, G.-K., Tignor, M., Allen, S. K., Boschung, J., Nauels, A., Xia,
345 Y., Bex, V., and Midgley, P. M., Cambridge University Press, Cambridge, United Kingdom
346 and New York, NY, USA., 2013.
- 347 Cox, P. M., Huntingford, C., and Williamson, M. S.: Emergent constraint on equilibrium climate
348 sensitivity from global temperature variability, *Nature*, 553, 319-322,
349 10.1038/nature25450, 2018.
- 350 Dee, D. P., et al.: The ERA-Interim reanalysis: Configuration and performance of the data
351 assimilation system, *Q. J. R. Meteor. Soc.*, 137, 553-597, 10.1002/qj.828, 2011.
- 352 Dessler, A. E., and Zelinka, M. D.: Climate feedbacks, in: *Encyclopedia of Atmospheric Sciences*,
353 edited by: North, G. R., Pyle, J., and Zhang, F., Elsevier, 18-25, 2014.
- 354 Forster, P. M.: Inference of climate sensitivity from analysis of Earth's energy budget, *Annual*
355 *Review of Earth and Planetary Sciences*, 44, 85-106, 10.1146/annurev-earth-060614-
356 105156, 2016.
- 357 Forster, P. M., et al.: Recommendations for diagnosing effective radiative forcing from climate
358 models for CMIP6, *J. Geophys. Res.*, 121, 12460-12475, 10.1002/2016jd025320, 2016.
- 359 Giorgetta, M. A., et al.: Climate and carbon cycle changes from 1850 to 2100 in MPI-ESM
360 simulations for the Coupled Model Intercomparison Project phase 5, *Journal of Advances in*
361 *Modeling Earth Systems*, 5, 572-597, 10.1002/jame.20038, 2013.

362 Gregory, J. M., Stouffer, R. J., Raper, S. C. B., Stott, P. A., and Rayner, N. A.: An observationally
363 based estimate of the climate sensitivity, *J. Climate*, 15, 3117-3121, 10.1175/1520-
364 0442(2002)015<3117:aobeot>2.0.co;2, 2002.

365 Gregory, J. M., et al.: A new method for diagnosing radiative forcing and climate sensitivity,
366 *Geophys. Res. Lett.*, 31, 10.1029/2003gl018747, 2004.

367 Gregory, J. M., and Andrews, T.: Variation in climate sensitivity and feedback parameters during
368 the historical period, *Geophys. Res. Lett.*, 43, 3911-3920, 10.1002/2016GL068406, 2016.

369 Hansen, J., et al.: Efficacy of climate forcings, *Journal of Geophysical Research: Atmospheres*,
370 110, n/a-n/a, 10.1029/2005JD005776, 2005.

371 Hansen, J., Ruedy, R., Sato, M., and Lo, K.: Global surface temperature change, *Rev. Geophys.*,
372 48, 10.1029/2010rg000345, 2010.

373 Huber, M., Beyerle, U., and Knutti, R.: Estimating climate sensitivity and future temperature in
374 the presence of natural climate variability, *Geophys. Res. Lett.*, 41, 2086-2092,
375 10.1002/2013GL058532, 2014.

376 Kummer, J. R., and Dessler, A. E.: The impact of forcing efficacy on the equilibrium climate
377 sensitivity, *Geophys. Res. Lett.*, 41, 3565-3568, 10.1002/2014gl060046, 2014.

378 Lewis, N., and Curry, J. A.: The implications for climate sensitivity of AR5 forcing and heat
379 uptake estimates, *Climate Dynamics*, 45, 1009-1023, 10.1007/s00382-014-2342-y, 2015.

380 Loeb, N. G., et al.: Toward optimal closure of the Earth's top-of-atmosphere radiation budget, *J.*
381 *Climate*, 22, 748-766, 10.1175/2008jcli2637.1, 2009.

382 Mauritsen, T., et al.: Developments in the MPI-M Earth System Model version 1.2 (MPI-
383 ESM1.2), in preparation, 2018.

384 Murphy, D. M.: Constraining climate sensitivity with linear fits to outgoing radiation, *Geophys.*
385 *Res. Lett.*, 37, 10.1029/2010GL042911, 2010.

386 Otto, A., et al.: Energy budget constraints on climate response, *Nature Geoscience*, 6, 415-416,
387 10.1038/ngeo1836, 2013.

388 Richardson, M., Cowtan, K., Hawkins, E., and Stolpe, M. B.: Reconciled climate response
389 estimates from climate models and the energy budget of Earth, *Nature Clim. Change*, 6,
390 931-935, 10.1038/nclimate3066, 2016.

391 Rose, B. E. J., and Rayborn, L.: The effects of ocean heat uptake on transient climate sensitivity,
392 *Current Climate Change Reports*, 2, 190-201, 10.1007/s40641-016-0048-4, 2016.

393 Rugenstein, M. A. A., Caldeira, K., and Knutti, R.: Dependence of global radiative feedbacks on
394 evolving patterns of surface heat fluxes, *Geophys. Res. Lett.*, 43, 9877-9885,
395 10.1002/2016GL070907, 2016.

396 Santer, B. D., et al.: Statistical significance of trends and trend differences in layer-average
397 atmospheric temperature time series, *J. Geophys. Res.*, 105, 7337-7356,
398 10.1029/1999jd901105, 2000.

399 Senior, C. A., and Mitchell, J. F. B.: The time-dependence of climate sensitivity, *Geophys. Res.*
400 *Lett.*, 27, 2685-2688, 10.1029/2000GL011373, 2000.

401 Shindell, D. T.: Inhomogeneous forcing and transient climate sensitivity, 4, 274,
402 10.1038/nclimate2136, 2014.

403 Skeie, R. B., Berntsen, T., Aldrin, M., Holden, M., and Myhre, G.: A lower and more constrained
404 estimate of climate sensitivity using updated observations and detailed radiative forcing
405 time series, *Earth System Dynamics*, 5, 139-175, 10.5194/esd-5-139-2014, 2014.

406 Spencer, R. W., and Braswell, W. D.: On the diagnosis of radiative feedback in the presence of
407 unknown radiative forcing, *J. Geophys. Res.*, 115, 10.1029/2009JD013371, 2010.

408 Stevens, B., Sherwood, S. C., Bony, S., and Webb, M. J.: Prospects for narrowing bounds on
409 Earth's equilibrium climate sensitivity, *Earth's Future*, 4, 512-522, 10.1002/2016EF000376,
410 2016.

411 Taylor, K. E., Stouffer, R. J., and Meehl, G. A.: An overview of CMIP5 and the experiment design,
412 *Bull. Am. Met. Soc.*, 93, 485-498, 10.1175/bams-d-11-00094.1, 2012.

413 Trenberth, K. E., Zhang, Y., Fasullo, J. T., and Taguchi, S.: Climate variability and relationships
414 between top-of-atmosphere radiation and temperatures on Earth, *J. Geophys. Res.*,
415 10.1002/2014JD022887, 2015.

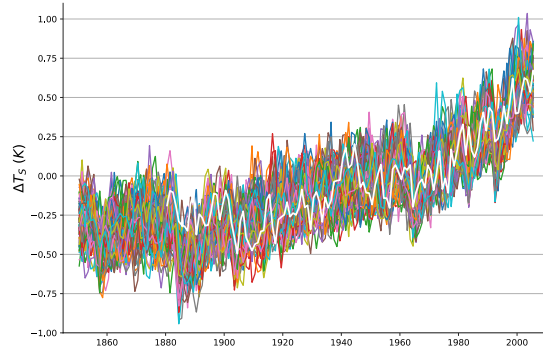
416 Wu, Q., and North, G. R.: Climate sensitivity and thermal inertia, *Geophys. Res. Lett.*, 29,
417 10.1029/2002GL014864, 2002.

418 Zhou, C., Zelinka, M. D., and Klein, S. A.: Impact of decadal cloud variations on the Earth's
419 energy budget, *Nature Geosci*, 9, 871-874, 10.1038/ngeo2828, 2016.

420 Zhou, C., Zelinka, M. D., and Klein, S. A.: Analyzing the dependence of global cloud feedback on
421 the spatial pattern of sea surface temperature change with a Green's function approach,
422 *Journal of Advances in Modeling Earth Systems*, 9, 2174-2189, 10.1002/2017MS001096,
423 2017.

424

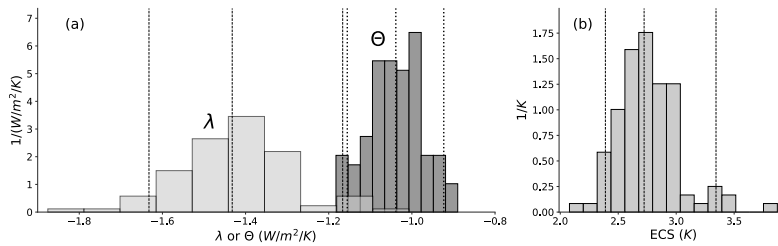
425



426

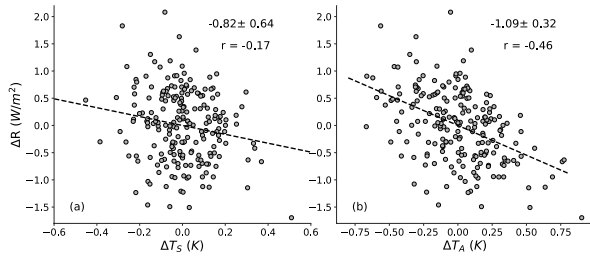
427 Fig. 1. Plot of annual and global average surface temperature from the 100 members of the
 428 MPI-ESM1.1 ensemble (colored lines), along with the GISTEMP measurements (Hansen et
 429 al., 2010) (white line). Temperatures are referenced to the 1951-1980 average.

430



431

432 Figure 2. PDFs of (a) λ (lighter) and Θ (darker) and (b) ECS derived from the members of the
 433 MPI-ESM1.1 historical ensemble. The vertical lines are the 5th, 50th, and 95th percentile of each
 434 distribution.



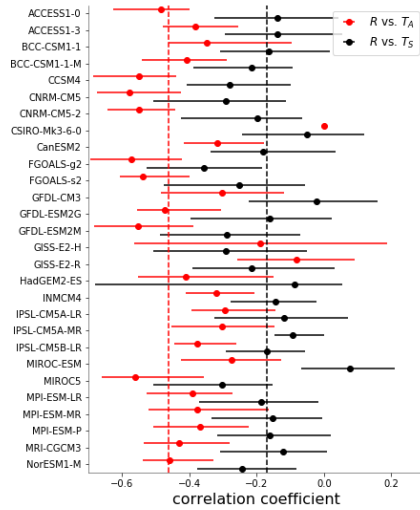
435

436 Figure 3. Scatter plot of detrended monthly anomalies of ΔR vs. (a) global average surface
 437 temperature ΔT_S , (b) tropical average 500-hPa temperature ΔT_A . Observations cover the period
 438 March 2000–July 2017 and anomalies are deviations from the mean annual cycle. The dashed
 439 lines are ordinary least-squares fits; the slope, 5-95% confidence interval, and correlation
 440 coefficient are shown on each panel. Confidence intervals account for autocorrelation of the
 441 time series (Santer et al., 2000).

Deleted: Jan.

442

443



445

446

447

448

449

450

451

Fig. 4. Correlation coefficients between ΔR and temperature in CMIP5 control runs: black and red symbols represent the correlation with ΔT_S and ΔT_A , respectively. The dot is the average of the correlation coefficients from the 17-year segments of the model run; the bars indicate the maximum and minimum values from the control run. The dashed lines are the corresponding correlation coefficients from the CERES regressions in Fig. 2.

Deleted: ΔT_S

Deleted: 6

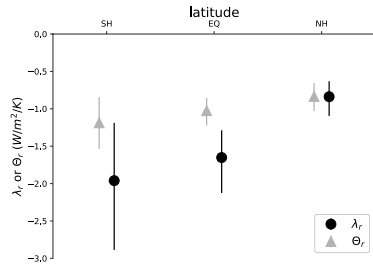
Deleted: blue

Deleted: is

Deleted: the average of the CMIP5 models, while the red dashed line is

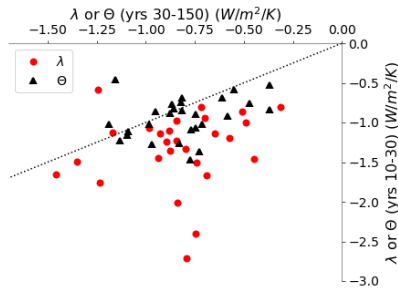
Deleted: a

459



460

461 Fig. 5. λ_r and Θ_r calculated as regional average $\Delta(R-F)$ divided by regional average temperature
 462 (ΔT_S for λ and ΔT_A for Θ). The regions are 90°S-19.4°S (SH), 19.4°S-19.4°N (EQ), and 19.4°N-
 463 90°N (NH). The values are calculated for each member of the 100-member ensemble; the solid
 464 symbols are the ensemble average while the bars show the 5-95% range.

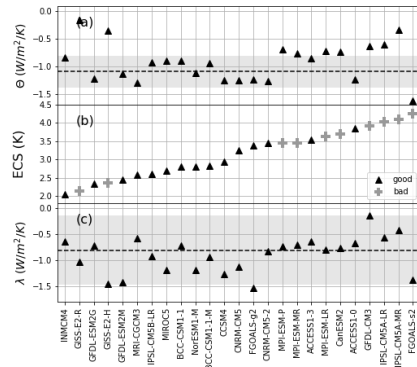


465

466 Fig. 6. Scatterplot of λ_{10-30} vs. λ_{30-150} (red circles) in CMIP5 abrupt4xCO₂ runs, as well as
 467 Θ_{10-30} vs. Θ_{30-150} (black triangles) in the same models. Each point represents one model.
 468 The dotted line is the 1:1 line. The subscripts (10-30, 30-150) indicate the years of the run
 469 from which the values are calculated.

Deleted: gray

Deleted: crosses



472

473

474

475

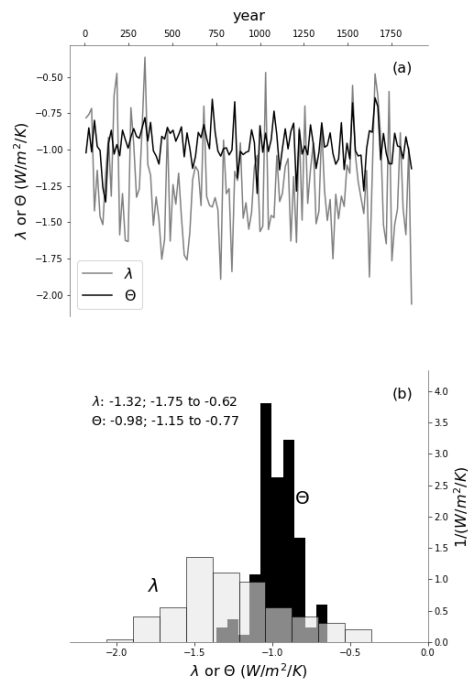
476

477

478

Figure 7. (a) Θ from individual CMIP5 control runs. The dotted line is the estimate from CERES observations; the gray region is the 5-95% confidence band. (b) ECS from each CMIP5 model, estimated from the first 150 years of abrupt $4\times\text{CO}_2$ runs using the Gregory method (Gregory et al., 2004). “Good” models are those whose Θ agrees with observations in panel (a), “bad” models are those that do not. (c) Same as panel (a), but for λ .

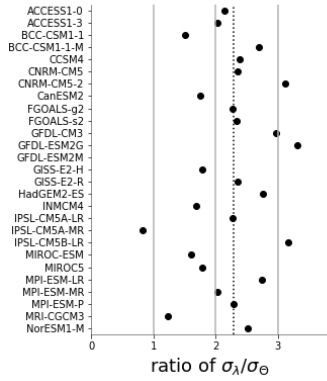
Deleted: (calculation described in the Appendix)



480

481 Fig. 8. (a) Time series of λ (gray) and Θ (black) estimated in a 17-year sliding window of a
 482 2000-year control run of the MPI-ESM1.1. (b) PDFs of the time series in panel a. Median
 483 and 5-95% confidence interval for each distribution is displayed on the plot.

Deleted: 6



485

486 Fig. 9. The standard deviation of the λ time series divided by the standard deviation of the

487 Θ time series. Each time series is calculated from 17-year segments of CMIP5 control runs.

488 The dotted line is the ensemble average.

489

Deleted: 6